JOURNAL OF THERMOPHYSICS AND HEAT TRANSFER
Vol. 13, No. 3, July–September 1999

Transient Thermal Analysis for Heating a Translucent Wall with Opaque Radiation Barriers

Robert Siegel*
NASA John H. Glenn Research Center at Lewis Field, Cleveland, Ohio 44135

The transient analysis of thermal behavior in translucent media including radiative transfer becomes computationally complex for a multiple-layer composite. A convenient method is developed here for analyzing combined radiation and conduction in a composite wall of translucent and opaque layers. The translucent layers transfer radiation by combined transmission, absorption, emission, and scattering. Metal layers can be required for strength of the composite or to protect ceramic surfaces from a reactive environment. Opaque layers within a translucent ceramic can be used to decrease radiant transmission that may degrade the ceramic insulating ability. The two-flux method is used to determine the local heat source produced by radiation in the translucent layers. The differential equation for the radiative flux in the two-flux method is solved with Green's functions that include the opaque or translucent boundary conditions of each translucent layer. Finite difference relations are derived for the transient energy equation, such that the calculated temperature distributions provide good accuracy for energy conservation during the transient. The solution technique is applied to illustrate radiation effects in a composite with one or two translucent layers, with and without opaque layers at the outer boundaries, or between the translucent layers.

Nomenclature

a = absorption coefficient of translucent material such as a ceramic, m^{-1}
B_0, B_1 = quantities, $2R_i/3\kappa_D$, $2R_m/3\kappa_D$
C, D = coefficients in homogeneous solution for $\tilde{G}$
C_{mc} = property ratio, $\rho_m c_m/\rho_c c_c$
c_c, c_m = specific heats of translucent material and of metal or opaque material, J/kg K
G = flux quantity in the two-flux method, W/m^2; $\tilde{G}$ is $G/\sigma T_i^4$
G_h = homogeneous part of the G function, W/m^2; $\tilde{G}_h$ is $G_h/\sigma T_i^4$
g_1, g_2 = Green's functions for radiative heat source in translucent material
H = dimensionless parameter, $h/\sigma T_i^3$
h_1, h_2 = convective heat transfer coefficients at outside surfaces of composite (Fig. 1), W/m^2 K
k_c, k_m = thermal conductivities of translucent material and of metal or opaque material, W/m K
m = quantity, $\kappa_D[3(1-\Omega)]^{1/2}$
N_c = conduction–radiation parameter, $k_c/4\sigma T_i^3\delta_c$
n = refractive index of translucent material
q_r = radiative flux in x direction, W/m^2; $\tilde{q}_r$ is $q_r/\sigma T_i^4$
q_{tot} = total energy transfer at steady state by combined radiation and conduction, W/m^2
$\tilde{q}1_r$, $\tilde{q}2_r$ = dimensionless radiation fluxes within first and second translucent layers
q_{r1}, q_{r2} = external radiation fluxes incident on outer surfaces of composite (Fig. 1), W/m^2
$\tilde{q}_{r1}$, $\tilde{q}_{r2}$ = dimensionless radiation fluxes, $q_{r1}/\sigma T_i^4$ and $q_{r2}/\sigma T_i^4$
R_i, R_o = quantities, $(1+\rho_i)/(1-\rho_i)$, $(1-\rho_o)/(1-\rho_i)$
R_m = quantity, $(2-\epsilon_{mi})/\epsilon_{mi}$
T = absolute temperature, K
T_{g1}, T_{g2} = gas temperatures for convection at outer boundaries (Fig. 1), K; t_g is T_g/T_i
T_i = initial uniform temperature (used as a reference temperature), K
T_{s1}, T_{s2} = temperatures of blackbody radiative surroundings at two sides of composite, K
t = dimensionless temperature, T/T_i
x = coordinate in a translucent layer (Fig. 1), m; X is x/δ_c
δ_c, δ_m = thicknesses of translucent coating and of metal or opaque material, m
ϵ_{mi}, ϵ_{mo} = emissivities of metal or opaque layer at inner and outer surfaces; Figs. 1b–1d
θ = time, s
κ = optical coordinate, $(a+\sigma_s)x$
κ_D = optical thickness of translucent layer, $(a+\sigma_s)\delta_c$
ρ_c, ρ_m = densities of translucent coating and of metal or opaque material, kg/m^3
ρ_o, ρ_i = external and internal reflectivities at a translucent boundary; Fig. 1a
σ = Stefan–Boltzmann constant, W/m^2 K^4
σ_s = scattering coefficient in translucent material, m^{-1}
υ = dimensionless time, $(4\sigma T_i^3/\rho_c c_c \delta_c)\theta$
Ω = scattering albedo of translucent material, $\sigma_s/(a+\sigma_s)$

Subscripts

c = translucent layer such as a ceramic
g = gas
h = homogeneous solution
j, k = grid points in translucent layers, where j is $0, \ldots, J$, k is $0, \ldots, K$ (Fig. 2)
m = metal or opaque layer
n = time increment

Introduction

SOME ceramics, such as zirconia, that may be used for high-temperature applications, such as in turbine engine combustors and diesel engines, are partially transparent for radiative energy transfer.[1,2] At elevated temperatures, the temperature distributions and heat flows in these ceramics can be affected by internal emission and by absorption and scattering of incident radiation. As temperatures are raised to obtain higher engine efficiencies, internal radiative transfer effects are increased and may need to be considered in more detail. Radiative transfer can act as an apparent increase in thermal conductivity that can degrade the effectiveness of a high-temperature

Received 14 December 1998; revision received 5 February 1999; accepted for publication 5 February 1999.

*Senior Research Scientist, Research and Technology Directorate, 21000 Brookpark Road; robert.siegel@grc.nasa.gov. Fellow AIAA.

ceramic insulating material. It is necessary to quantitatively estimate the radiation effects for both steady and unsteady conditions and if necessary provide a means for reducing radiative transfer.

A possible reduction method is to place opaque radiation shields within the ceramic, such as thin metal layers with a high melting temperature. Metal layers might also be used at outer surfaces as protection of the ceramic from corrosive combustion gases and for structural support. The result is a composite of translucent and opaque layers. For some applications, transient temperature responses to variable heating are needed for evaluating thermal performance and stresses. The radiative effects on transient responses can be complex in a high-temperature composite where there is large internal emission and multiple reflections between boundaries. For translucent materials, numerical procedures are usually used to solve the transient energy equation coupled with the radiative transfer relations.[3] The computations become more extensive as the number of translucent layers is increased in the composite.[4–6]

This paper develops a convenient analytical and numerical procedure for obtaining transient temperature distributions within composites of translucent and opaque layers. Finite difference relations are developed to solve the energy equation for transient temperatures in the translucent layers and to include the heat capacity of the opaque layers. At each time step the solution requires the local heat source produced by radiative transfer in each translucent layer. In the literature, both exact and approximate formulations have been used to evaluate the radiative contribution. With general external conditions of convection and radiative exchange for a translucent layer with diffuse surfaces, it has been found that the two-flux method yields temperature distributions that compare well with those from more exact methods. This includes large scattering as needed for a ceramic material such as zirconia.[7]

The two-flux method is used here, and, for simplicity, isotropic scattering is assumed. The two-flux equations provide a second-order differential equation that must be solved to evaluate the internal radiative source in each translucent layer at each time. The differential equation is solved here by using Green's functions.[8] Three Green's functions are employed to account for the various boundary conditions that must be satisfied for the solution in each translucent layer. Relations are provided for boundaries where the translucent layer has an adjacent opaque layer and for a translucent layer without an opaque layer on one or both boundaries so that radiation can pass through an exposed translucent boundary.

Illustrative results for heating a composite demonstrate the transient behavior when translucent layers are present as compared with all layers being opaque. For the opaque limit, radiant absorption and emission occur only at the external surfaces. The heating of a translucent layer with translucent boundaries is contrasted with that of a translucent layer with a thin opaque layer at one or both of its boundaries. The effect is also shown of placing a thin opaque layer between two translucent layers.

Analysis

The geometry consists of translucent layers combined with thin opaque metal layers in composites as shown in Figs. 1a–1d. The solution method is applied for these geometries, but the relations are valid for a larger number of layers. Illustrative numerical results are obtained for a translucent layer that is bare on both sides, a translucent layer with a thin opaque layer on one side, a translucent layer with a thin opaque layer on each side, and two translucent layers with an opaque layer between them and with an opaque layer at each external boundary. Each translucent layer is an absorbing dielectric material that is heat conducting, has a refractive index larger than one, and is assumed isotropically scattering, gray, and with diffuse boundaries. For the illustrative results here, all of the translucent layers in a composite have the same properties. To begin a transient, each external boundary is exposed to radiative surroundings and to convection by a transparent gas. Transient temperature distributions are obtained, and results at steady state are compared with independent steady-state calculations using the methods in Refs. 7–9. The gray relations given here can be extended to nongray properties, as done for steady solutions in Ref. 9.

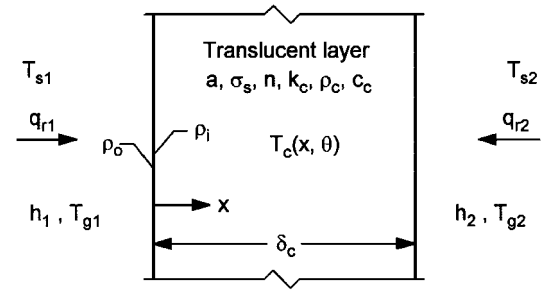

a) Translucent layer with exposed boundaries

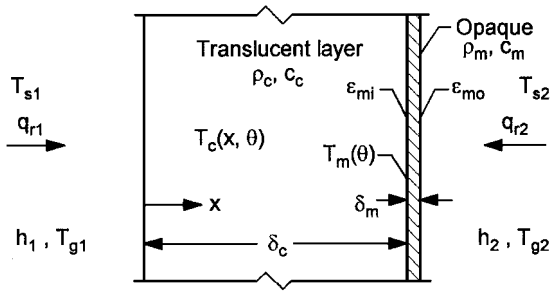

b) Translucent layer with thin opaque layer at one boundary

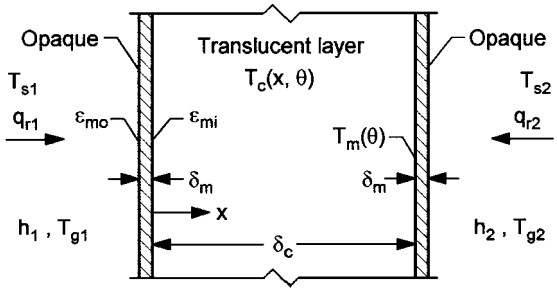

c) Translucent layer with thin opaque layer at both boundaries

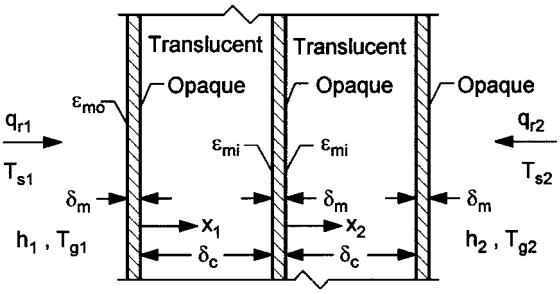

d) Two translucent layers with opaque layer between them and at outer boundaries

Fig. 1 Geometry and nomenclature for transient radiation and conduction in single and composite layers of translucent and opaque materials with external boundaries subjected to radiation and convection.

Energy Equation and Two-Flux Relations for Translucent Layer

The transient energy equation will be solved in each translucent layer. Each opaque layer is assumed to be thin and to have a sufficiently high thermal conductivity that it has a uniform temperature distribution at any time. The heat capacity of each opaque layer is included, and its temperature is assumed equal to the temperature of the adjacent boundary of the translucent material. These assumptions are incorporated into the finite difference relations developed in Appendix B. The dimensionless energy equation for transient temperatures in each translucent layer for constant thermal properties is[10]

$$\frac{\partial t_c}{\partial \upsilon} = N_c \frac{\partial^2 t_c}{\partial X^2} - \frac{1}{4}\frac{\partial \tilde{q}_r}{\partial X} \tag{1}$$

The $-(\frac{1}{4})\partial\tilde{q}_r(X, \upsilon)/\partial X$ term is the local heat source from radiative transfer, including effects of interactions with the boundaries. It is obtained from two-flux relations in terms of the instantaneous temperature distribution in the layer and the surrounding radiative conditions. The two-flux equations are[7]

$$\frac{\partial\tilde{q}_r(X, \upsilon)}{\partial X} = \kappa_D(1-\Omega)\left[4n^2t_c^4(X, \upsilon) - \tilde{G}(X, \upsilon)\right] \tag{2a}$$

$$\frac{\partial\tilde{G}(X, \upsilon)}{\partial X} = -3\kappa_D\tilde{q}_r(X, \upsilon) \tag{2b}$$

Boundary and Initial Conditions

As shown in Fig. 1, each boundary of a translucent layer is either exposed directly to the surroundings or is bounded by an opaque material. For a gray translucent layer with a translucent boundary, there is no radiative absorption at the plane of the boundary because radiative interaction requires a volume of material and the boundary itself has no volume. Hence, for a translucent boundary exposed to external radiation and convection, the boundary condition is a balance of only convection and conduction so that at $x = 0$ and δ_c in Fig. 1a the conditions in dimensionless form are

$$-4N_c\frac{\partial t_c}{\partial X}\bigg|_{X=0} = H_1[t_{g1} - t_c(0, \upsilon)] \tag{3a}$$

$$4N_c\frac{\partial t_c}{\partial X}\bigg|_{X=1} = H_2[t_{g2} - t_c(1, \upsilon)] \tag{3b}$$

If there are opaque boundaries at $x = 0$ and δ_c, as in Fig. 1c or 1d, the assumption is made that each thin opaque layer has a sufficiently high conductivity, such as for a metal, that its temperature is uniform and is equal to that of the adjacent translucent material. The boundary conditions then equate the conduction into the translucent layer and the rate of internal energy increase of the thin opaque layer to the convection supplied to the external boundary of the opaque layer and the radiation absorbed at both the external and internal opaque boundaries, where the surface properties of the opaque layer are assumed gray. Because the net radiative flux in the translucent material is not transmitted into the opaque layer, the radiative flux provides the radiative energy absorption in the opaque layer at the interface with the translucent layer. This energy balance is discussed in more detail in Appendix B, where the finite difference relations are formulated. The resulting boundary conditions are

$$-4N_c\frac{\partial t_c}{\partial X}\bigg|_{X=0} + 4C_{mc}\frac{\delta_m}{\delta_c}\frac{\partial t_c(0, \upsilon)}{\partial\upsilon} = H_1[t_{g1} - t_c(0, \upsilon)] + \epsilon_{mo}\left[\tilde{q}_{r1} - t_c^4(0, \upsilon)\right] - \tilde{q}_r(0, \upsilon) \tag{4a}$$

$$4N_c\frac{\partial t_c}{\partial X}\bigg|_{X=1} + 4C_{mc}\frac{\delta_m}{\delta_c}\frac{\partial t_c(1, \upsilon)}{\partial\upsilon} = H_2[t_{g2} - t_c(1, \upsilon)] + \epsilon_{mo}\left[\tilde{q}_{r2} - t_c^4(1, \upsilon)\right] + \tilde{q}_r(1, \upsilon) \tag{4b}$$

For Fig. 1b, where there is one transparent and one opaque boundary, conditions (3a) and (4b) are used.

Boundary conditions must also be provided for solving the two-flux equations (2a) and (2b) for evaluating the local radiative heat source term for use in Eq. (1). Considering incident and reflected fluxes at an interface of a translucent material, and emission, absorption, and reflection by an adjacent opaque layer, radiative boundary relations were developed in Ref. 8 for a translucent layer with a clean exposed boundary and with a boundary that is at the interface with an opaque substrate. For a clean boundary at $x = 0$ that is directly exposed to the surrounding radiative environment,

$$\tilde{G}(0, \upsilon) - \frac{2R_i}{3\kappa_D}\frac{\partial\tilde{G}}{\partial X}\bigg|_{X=0} = 4R_o\tilde{q}_{r1} \tag{5a}$$

For a boundary such as at $x = \delta_c$ in Fig. 1b, corresponding to $X = 1$,

$$\tilde{G}(1, \upsilon) + \frac{2R_m}{3\kappa_D}\frac{\partial\tilde{G}}{\partial X}\bigg|_{X=1} = 4n^2t_c^4(1, \upsilon) \tag{5b}$$

For a transient solution, initial temperatures must be specified in the composite. The initial condition for the present results is a uniform temperature T_i in all translucent and opaque layers, $T_c(x, \theta = 0) = T_m(\theta = 0) = T_i$. Nonuniform initial temperatures could also be used, where T_i in the analysis would then be selected as any convenient reference value that characterizes the range of initial temperatures.

Green's Function for $\partial\tilde{q}_r(X, \tau)/\partial X$

By combining Eqs. (2a) and (2b) to eliminate $\tilde{q}_r$ and by letting $m = \kappa_D[3(1-\Omega)]^{1/2}$, a differential equation is obtained for the $G(x, \theta)$ function in each translucent layer,

$$\frac{d^2\tilde{G}}{dX^2} - m^2\tilde{G}(X, \upsilon) = -4m^2n^2t_c^4(X, \upsilon) \tag{6}$$

This was solved by developing Green's functions for Eq. (6) using the types of boundary conditions as in Eqs. (5a) and (5b). There are three different Green's functions, as derived in Refs. 7–9, for the conditions of both translucent boundaries exposed directly to a radiative environment, one translucent boundary exposed and the other adjacent to an opaque layer, and a translucent layer contained between two opaque layers. The three Green's functions with their corresponding homogeneous solutions are summarized in Appendix A using a common notation. By using these functions, the general solution of Eq. (6) at each time is obtained by adding the homogeneous solution to the nonhomogeneous contribution evaluated by integrating the Green's function multiplied by $t_c^4(X, \upsilon)$: This yields

$$\tilde{G}(X, \upsilon) = \tilde{G}_h(X, \upsilon) + 4mn^2\left[\int_{\xi=0}^{X} g_2(X, \xi)t_c^4(\xi, \upsilon)\,d\xi + \int_{\xi=X}^{1} g_1(X, \xi)t_c^4(\xi, \upsilon)\,d\xi\right] \tag{7}$$

Finite Difference Relations and Numerical Evaluation

The transient energy equation must be solved for the layers in the composite with an internal heat source in each translucent layer. Solutions were obtained using finite difference relations as provided in Appendix B. As shown in Fig. 2, various difference equations are required at the boundaries of the translucent material to account for either a boundary that is clean and exposed or is in contact with a thin opaque layer at an outer boundary or internally (Fig. 2). Each opaque layer is sufficiently thin and of high conductivity so its temperature can be assumed uniform at each time. A finite difference equation is written for an arbitrary interior point in the translucent material, for a boundary point when the translucent boundary is directly exposed to the radiative and convective environment, for a point at an outer boundary of a translucent layer that is adjacent to a thin opaque metal layer, and for a boundary of the translucent material adjacent to a thin interior metal layer. The heat capacity of the thin opaque layers is incorporated into the finite difference formulations for the grid points at the interfaces of translucent and opaque layers.

To start a calculation, the radiative heat source in Eq. (1) is calculated from Eq. (2a) by evaluating $\tilde{G}(X, \upsilon)$ from Eq. (7) using the specified initial temperature. The required Green's function for Eq. (7) was evaluated from the appropriate relations in Appendix A for each translucent layer. In Eq. (7), the homogeneous solution in each layer was evaluated from Eqs. (A6–A9) in Appendix A. Double precision was used for all evaluations, and Romberg integration in an available computer subroutine was used for the integrals in Eq. (7). After advancing the temperatures each time increment by use of the finite difference equations, the radiative heat source was reevaluated

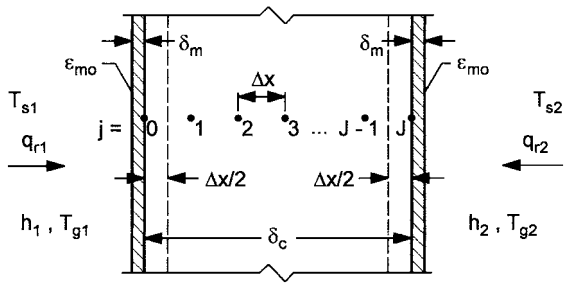

a) Opaque layer at each boundary of a translucent layer

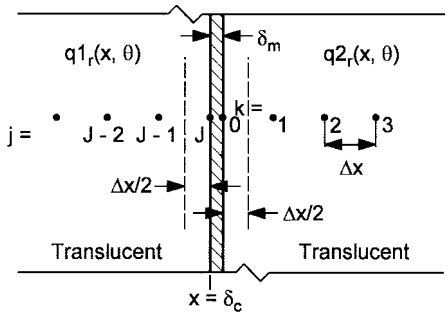

b) Opaque layer between two translucent layers

Fig. 2 Nomenclature for finite difference relations for a translucent material adjacent to an opaque layer.

from Eqs. (7) and (2a) using the new temperature distributions in each translucent layer.

For stability in the transient solution, the explicit finite difference method required small dimensionless time increments such as $\Delta\upsilon \approx 10^{-5}$ as estimated from the standard criterion for the transient heat conduction equation. It was found that 20 spatial increments in a single translucent layer, or 10 increments in each of two translucent layers, gave good accuracy as tested by reducing increment size to one-half and time step size to one-quarter to retain stability. An overall heat balance was made for each time step to compare the sum of incident radiation and convection to the boundaries of the composite, with the total of radiation leaving the composite and the change in the composite internal energy; the balance was within a few tenths of 1% using the finite difference relations developed here.

To compare with the steady-state limit approached by the transient solution, the temperature distribution at steady state was evaluated independently, and very good agreement was obtained. The basic procedure used for the independent steady-state method is the same for the various configurations in Fig. 1, but the details differ to allow for having various opaque barriers. The procedures for steady-state solutions are in Refs. 8 and 9.

Results and Discussion

An analytical and numerical procedure was developed to obtain the transient thermal response of a composite wall composed of one or more translucent layers separated by opaque radiation barriers, and with or without opaque layers at the external boundaries. Radiative heating within each translucent region was evaluated by solving a two-flux differential equation by using Green's functions that incorporate the radiative boundary conditions for either a clean exposed translucent boundary or a translucent material adjacent to an opaque radiation barrier. Explicit finite difference relations for the transient energy equation were derived to include radiative effects at the interfaces of the translucent and opaque layers along with the heat capacity of the opaque material.

The transient solutions that will be shown are to demonstrate the method and illustrate some of the transient heating characteristics when a material is translucent as compared with being opaque. For transients in a composite, there are many independent quantities such as the material properties including the density and heat capacity, the radiative and convective heating at the boundaries, the surface emissive properties of the opaque layers, and the optical properties of the translucent materials. Consequently, it is not feasible to do a parametric study of all of the variables involved. The primary objective of this paper is to provide a method that can be used for design studies to evaluate the significance of some composite layers being translucent. The densities and heat capacities selected for illustration are like those for zirconia and stainless steel, and the refractive index is like that for zirconia. The optical thickness of the layers was such that radiation in them would be significant, and the possible importance of radiation would, therefore, be demonstrated. The physical thicknesses of the translucent material was chosen as 2 mm, and the opaque barriers that are considered to be thin metal layers in the examples that follow are 0.1 mm thick. The heat transfer coefficients and temperatures are in the ranges for turbine engine combustion chambers.

The temperatures in Fig. 3a show the transient response of an opaque layer 2 mm thick with the thermal properties of zirconia and without any metal layers at its boundaries (Fig. 1a); these are the same thermal properties as for the translucent layers in Figs. 4–6. The surface reflection properties were obtained using the Fresnel equations assuming diffuse interfaces with a refractive index of $n = 2$ for zirconia. The parameters (Fig. 3) are as follows: $\delta_c = 2$ mm, $k_c = 0.8$ W/m K, $c_c = 570$ J/kg K, $\rho_c = 5200$ kg/m^3, $h_1 = h_2 = 250$ W/m^2 K, $T_i = 300$ K, $T_{s1} = T_{g1} = 2000$ K, and $T_{s2} = T_{g2} = 300$ K. Starting at a uniform temperature of $T_i = 300$ K, the layer was exposed to a 2000 K black environment and to convecting gas at 2000 K on the side at $x = 0$. The side at $x = \delta_c$ is cooled by radiation in a 300 K black environment and by convecting gas at 300 K. With the layer opaque, there is only internal heat conduction, but radiation is present to and from the boundaries. The times during the transient in Fig. 3a are given in seconds. The onset of the transient provides rapid heating at and near $x = 0$, with the region near $x = \delta_c$ being much slower to respond. At larger times, the transient distributions gradually change toward a linear shape, and the linear steady-state temperature distribution is approached after 20 s of heating. These results are for comparison with Figs. 3b–6.

For Fig. 3b the same conditions are used as in Fig. 3a with the layer in Fig. 1a now made translucent with gray properties, no scattering, and an optical thickness of $\kappa_D = a\delta_c = 2$. With radiative penetration through the boundary $x = 0$ from the 2000 K black surroundings, the temperatures in the region near $x = 0$ rise more slowly, but radiant transmission increases heating near the boundary at $x = \delta_c$. Compared with Fig. 3a, translucence reduces the temperature gradients in the layer as a result of the augmented ability for energy transport by radiative transfer and by internal reflections that tend to distribute energy across the layer. The approach to steady state is slightly more rapid than for the opaque layer in Fig. 3a as a result of radiant propagation into the layer to provide internal heating; this provides a faster time response compared with having only energy diffusion by heat conduction. The temperatures are approaching steady state after about 15 s. The temperatures reached in 20 s agree very well with those for steady state that were calculated independently using the method in Ref. 8 modified with the boundary relations in Ref. 7. The steady-state temperature distribution for an opaque layer is included from Fig. 3a. Translucence produces more uniform steady-state temperatures as a result of increased energy transfer ability in the layer by radiation added to heat conduction and by redistribution of energy by multiple internal reflections. The temperatures near $x = 0$ are decreased by translucence, but those near $x = \delta_c$ are increased. The steady-state heat transfer through the layer q_{tot} by combined radiation and conduction is also shown and compared with that for an opaque layer where there is radiation only at the boundaries. The heat transferred through the translucent layer is almost twice that for an opaque layer.

In Fig. 4 the translucent layer in Fig. 3 is modified by having a thin opaque layer on the cooled side that prevents radiation from being transmitted completely through the entire layer (Fig. 1b). The parameters (Fig. 4) are as follows: $\delta_c = 2$ mm, $\delta_m = 0.1$ mm, $k_c = 0.8$ W/m K, $k_m = 33$ W/m K, $c_c = 570$ J/kg K, $c_m = 460$ J/kg K, $\rho_c = 5200$ kg/m^3, $\rho_m = 7800$ kg/m^3, $n = 2$ ($\rho_i = 0.79015$, $\rho_o = 0.16060$), $a = 1000$ m^{-1}, $\sigma_s = 0$, $\epsilon_{mi} = 0.3$, $\epsilon_{mo} = 0.3$, $h_1 = h_2 = 250$ W/m^2 K, $T_i = 300$ K, $T_{s1} = T_{g1} = 2000$ K, and $T_{s2} = T_{g2} = 300$ K. For a bare

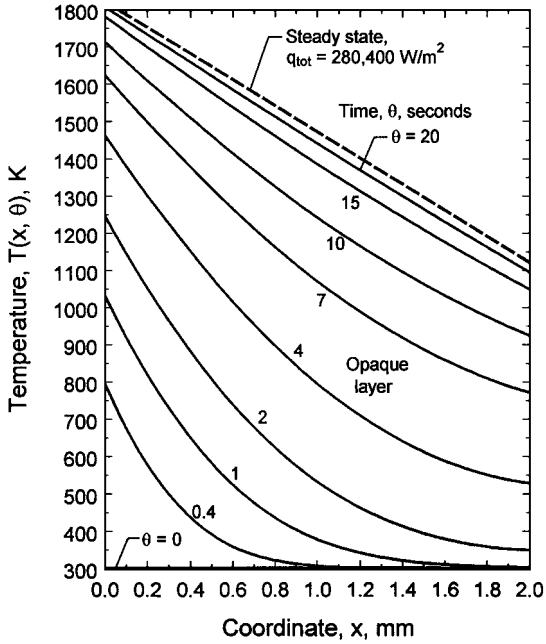

a) Limiting results for an opaque layer, no internal radiation

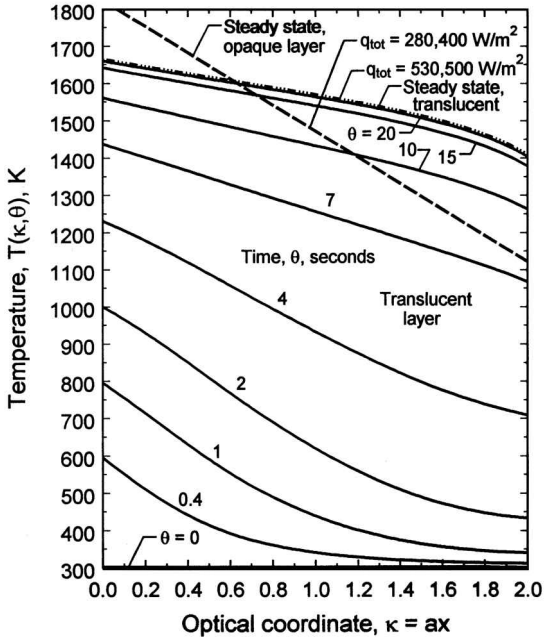

b) Results when layer is translucent, $n = 2$ ($\rho_i = 0.79015$, $\rho_o = 0.16060$), $a = 1000\ \mathrm{m}^{-1}$, $\sigma_s = 0$

Fig. 3 Transient temperatures in a single layer exposed to radiation and convection on both sides following suddenly applied heating at one side.

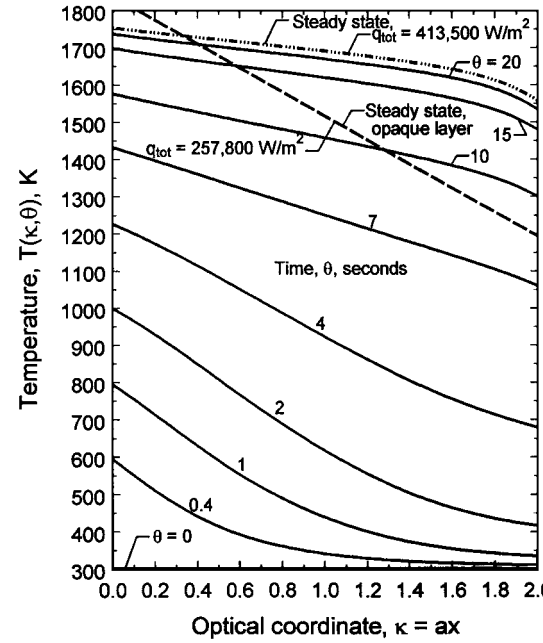

Fig. 4 Transient temperatures in a single translucent layer in a composite with a single opaque layer, exposed to radiation and convection on both sides following suddenly applied heating at the side without the opaque coating.

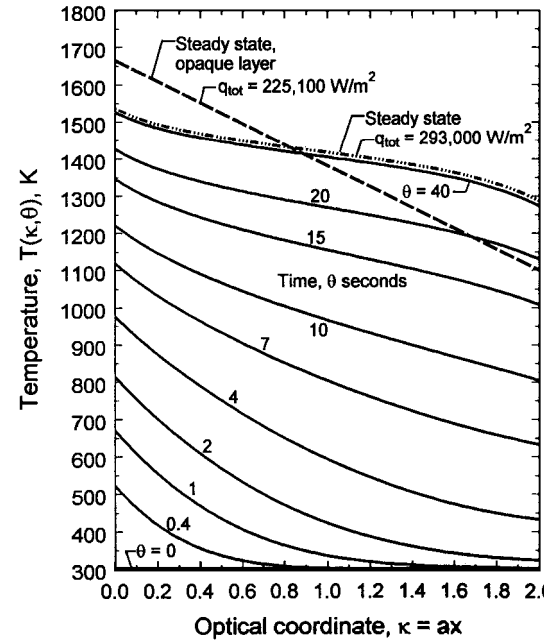

Fig. 5 Transient temperatures in a single translucent layer in a composite with an opaque layer at both boundaries, exposed to radiation and convection on both sides following suddenly applied heating at one side.

layer, the reflectivity from the inside of a translucent boundary is produced partly by ordinary reflection at the boundary and mostly by total internal reflections within the high index of refraction material; for $n = 2$ this gives $\rho_i = 0.790$ for a diffuse surface. For the thin metal layer, which was selected as stainless steel, the emissivity was chosen as $\epsilon_{mi} = 0.30$ so the reflectivity from the metal into the translucent material is $\rho_i = 1 - \epsilon_{mi} = 0.70$; hence, the extent of internal reflection has not been changed very much for comparing Figs. 3b and 4. The metal layer is $\frac{1}{20}$th of the thickness of the zirconia, and this adds a small heat capacity. The thin metal plate is not drawn on Fig. 4, but has the same instantaneous temperature as the translucent layer at $ax = 2$ corresponding to $x = \delta_c = 2$ mm. The steady-state temperature distribution for the opaque limit is changed somewhat from that in Fig. 3b because absorption and emission at the external surface of the metal (at $x = \delta_c + \delta_m$) with $\epsilon_{mo} = 0.3$ has replaced the translucent boundary at $x = \delta_c$ for the results in Fig. 3b. At steady state, the transient results are in very good agreement with the steady-state distribution calculated independently by using the method in Ref. 8; by extending to longer times, the transient and steady-state distributions coincide as in Fig. 3a. That radiant energy cannot pass through the material to the cooled environment because of blockage by the metal layer provides increased retention in the composite of energy provided by the high-temperature environment on the left side. This produces higher steady-state temperatures than in Fig. 3b. It also reduces the steady-state heat flow through the composite.

The change from Fig. 4 to 5 is that a second metal layer of the same thickness as for Fig. 4 at $ax = 2$ (at $x = \delta_c$) is now placed on the boundary at $x = 0$ so it is the metal layer that is exposed to the

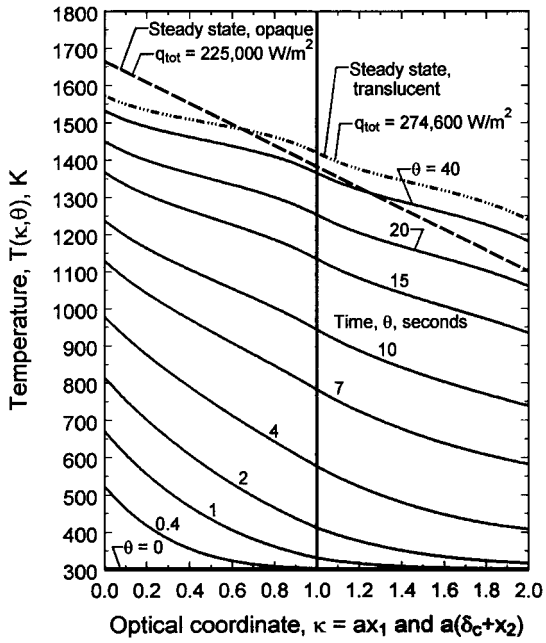

Fig. 6 Transient temperatures in a composite of two translucent layers with an opaque layer between them and with an opaque layer at each external boundary, exposed to radiation and convection on both sides following suddenly applied heating at one side.

incident radiation from the 2000 K black environment; this corresponds to Fig. 1c. The parameters (Fig. 5) are as follows: $\delta_c = 2$ mm, $\delta_m = 0.1$ mm, $k_c = 0.8$, $k_m = 33$, $c_c = 570$ J/kg K, $c_m = 460$ J/kg K, $\rho_c = 5200$ kg/m^3, $\rho_m = 7800$ kg/m^3, $n = 2$ ($\rho_i = 0.79015$, $\rho_o = 0.16060$), $a = 1000$ m^{-1}, $\sigma_s = 0$, $\epsilon_{mi} = 0.3$, $\epsilon_{mo} = 0.3$, $h_1 = h_2 = 250$ W/m^2 K, $T_i = 300$ K, $T_{s1} = T_{g1} = 2000$ K, and $T_{s2} = T_{g2} = 300$ K. Compared with a bare layer that has a reflectivity of $\rho_o = 0.161$ for a diffuse surface of a material with a refractive index of $n = 2$, the metal reflectivity is $1 - \epsilon_{mo} = 0.7$. Hence, the metal reflects away significant incident radiation, in addition to preventing direct passage of radiation into the layer from the hot environment. There are now opaque absorbing and emitting boundaries at both sides of the translucent layer. There is still significant radiation transport inside the translucent layer when its temperature becomes elevated, which produces temperature distributions that are much more uniform than in Fig. 3a, where there is only heat conduction. The dashed line for the steady-state distribution when the entire composite is made opaque is changed as a result of increased reflection of the incident radiation from the left side of the composite. This shielding effect by the metal layer on the high-temperature side of the composite reduces the transient response compared with Fig. 4 so that a longer time is required to approach steady state, and the steady-state temperatures are reduced. The steady-state heat transfer through the composite is also substantially reduced. At steady state, there is very good agreement with results calculated independently by using the steady-state method in Ref. 9.

For Fig. 6, the translucent layer has been divided into two equal thicknesses as in Fig. 1d. The parameters (Fig. 6) are as follows: $\delta_c = 1$ mm for each layer, $\delta_m = 0.1$ mm for each layer, $k_c = 0.8$, $k_m = 33$, $c_c = 570$ J/kg K, $c_m = 460$ J/kg K, $\rho_c = 5200$ kg/m^3, $\rho_m = 7800$ kg/m^3, $n = 2$ ($\rho_i = 0.79015$, $\rho_o = 0.16060$), $a = 1000$ m^{-1}, $\sigma_s = 0$, $\epsilon_{mi} = 0.3$, $\epsilon_{mo} = 0.3$, $h_1 = h_2 = 250$ W/m^2 K, $T_i = 300$ K, $T_{s1} = T_{g1} = 2000$ K, and $T_{s2} = T_{g2} = 300$ K. Each layer has an optical thickness of $\kappa_D = a\delta_c = 1$. Compared with the composite for Fig. 5, an additional metal shield has been placed along the centerplane of the composite between the two translucent layers (see Fig. 1d). The central shield blocks direct radiative transmission between the first and second translucent layers and compared with Fig. 5, which does not have an internal shield, the temperatures are increased in the first layer and reduced in the second layer. At steady state, the temperatures approach somewhat more closely to the limit when the entire composite is opaque. The steady-state temperature distribution in a composite of two translucent layers with three opaque radiation shields was calculated independently using the method in Ref. 9, where a steady-state analysis was developed for a composite of alternate translucent and opaque layers. The transient results are approaching that limit. The radiation shields are fairly effective for decreasing radiative transmission effects as would be desirable in ceramics used for protection from a high-temperature environment such as a liner in a turbine engine combustion chamber. The steady-state heat flow in Fig. 6 is somewhat reduced from that in Fig. 5.

Conclusions

A method was developed combining a Green's function solution and finite differences for transient thermal analysis of a composite incorporating translucent ceramic layers in a high-temperature environment. This is a possible design for a ceramic liner in a turbine engine combustion chamber. The translucent layers can be combined in the composite with thin metal layers used for surface protection, internal and external radiation shielding, and structural reinforcement. For the radiative heating and transport in the translucent layers, the two-flux equations were solved with a Green's function to obtain a radiative internal heat source in the transient energy equation. The Green's function analytically incorporates the radiative reflective boundary conditions for the translucent layer with and without metal layers at its boundaries. A finite difference method was used to solve the transient energy equation. Finite difference relations were derived to include radiative effects at the ceramic–metal interfaces and at the external boundaries and to include the heat capacity of the thin metal layers. The transient temperature distributions converged very well toward steady-state values obtained by an independent method.

The transient thermal behavior for heating a translucent layer by radiation and convection is compared with a layer without internal radiation effects, but with radiative absorption and reflection at its external surfaces. The effects of radiation shields at the external surfaces and inside the translucent material are demonstrated on transient heating, steady-state temperature distributions, and steady-state heat transfer through the composite. Translucence decreases transient temperature gradients and reduces the response of the material near the high-temperature source. A radiation shield at the hot side is effective in reducing temperature levels. A single shield at the cooled side increases retention of incident energy from the environment on the hot side. This raises temperatures compared with a translucent layer without a shield on its cooled side.

Appendix A: Green's Functions

Solutions for Eq. (6) in analytical form, which satisfy boundary conditions such as Eqs. (5a) and (5b), can be obtained by deriving Green's functions. There are three different cases for the translucent layers in the composites in Fig. 1. Case 1 is for both boundaries of the translucent layer exposed directly to the environment. Case 2 is for a translucent layer exposed to the environment on the left side and with an opaque layer on the right side. Case 3 is for a translucent layer with an opaque layer on both sides. Green's functions in terms of dimensionless variables have been derived in Refs. 7–9 for these conditions, and all of Green's functions have the same algebraic form with differing coefficients. The form is

$$g_1(X,\xi) = \left[\frac{\sinh m(1-\xi) + B_1 m \cosh m(1-\xi)}{\text{denom}}\right] \times (\sinh mX + B_0 m \cosh mX) \qquad 0 \le X < \xi \tag{A1a}$$

$$g_2(X,\xi) = \left[\frac{\sinh m\xi + B_0 m \cosh m\xi}{\text{denom}}\right][\sinh m(1-X) + B_1 m \cosh m(1-X)] \qquad \xi < X \le 1 \tag{A1b}$$

where the denominator term in Eqs. (A1a) and (A1b) is

$$\text{denom} = \left(1 + B_0 B_1 m^2\right)\sinh m + (B_0 + B_1) m \cosh m \tag{A2}$$

For case 1 with both boundaries translucent, B_0 and B_1 are equal and are given by

$$B_0 = B_1 = \frac{2}{3(a+\sigma_s)\delta_c}\frac{1+\rho_i}{1-\rho_i} \tag{A3}$$

For case 2, B_0 and B_1 are given by

$$B_0 = \frac{2}{3(a+\sigma_s)\delta_c}\frac{1+\rho_i}{1-\rho_i} \tag{A4a}$$

$$B_1 = \frac{2}{3(a+\sigma_s)\delta_c}\frac{2-\epsilon_{mi}}{\epsilon_{mi}} \tag{A4b}$$

For case 3 with both boundaries opaque, B_0 and B_1 are equal and are given by

$$B_0 = B_1 = \frac{2}{3(a+\sigma_s)\delta_c}\frac{2-\epsilon_{mi}}{\epsilon_{mi}} \tag{A5}$$

The functions $g_1(X, \xi)$ and $g_2(X, \xi)$ account for the nonhomogeneous term in Eq. (6) in the solution for $\tilde{G}(X, \upsilon)$ at each time. The homogeneous solution must be added to this to obtain the complete solution. For case 1, the homogeneous solution is given by[7]

$$\tilde{G}_h(X) = \frac{1-\rho_o}{1-\rho_i}\frac{4}{\text{denom}}\{[\sinh m(1-X) + B_0 m\cosh m(1-X)]\tilde{q}_{r1} + [\sinh mX + B_1 m\cosh mX]\tilde{q}_{r2}\} \tag{A6}$$

For cases 2 and 3, the homogeneous solution has the same form[8,9]:

$$\tilde{G}_h(X, \upsilon) = C(\upsilon)\cosh mX + D(\upsilon)\sinh mX \tag{A7}$$

For case 2, the coefficients are given by

$$C(\upsilon) = \frac{4}{\text{denom}}\Big[R_o(\sinh m + B_1 m\cosh m)\tilde{q}_{r1} + B_0 mn^2 t_c^4(X=1, \upsilon)\Big] \tag{A8a}$$

$$D(\upsilon) = \frac{C(\upsilon) - 4R_o\tilde{q}_{r1}}{B_0 m} \tag{A8b}$$

For case 3, the coefficients are found from

$$C(\upsilon) = \frac{4}{\text{denom}}\Big[(\sinh m + B_1 m\cosh m)n^2 t_c^4(X=0, \upsilon) + B_0 mn^2 t_c^4(X=1, \upsilon)\Big] \tag{A9a}$$

$$D(\upsilon) = \frac{C(\upsilon) - 4n^2 t_c^4(X=0, \upsilon)}{B_0 m} \tag{A9b}$$

Appendix B: Finite Difference Relations

The temperature distributions are advanced each $\Delta\upsilon$ with explicit finite difference relations. For an interior point at grid position j in the translucent material in Fig. 2a, Eq. (1) gives

$$t_{j,n+1} = t_{j,n} + \frac{N_c\Delta\upsilon}{\Delta X^2}(t_{j+1,n} - 2t_{j,n} + t_{j-1,n}) - \frac{\Delta\upsilon}{4}\frac{\partial\tilde{q}_r}{\partial X}\bigg|_{j,n} \tag{B1}$$

where n refers to the time increment.

To develop boundary relations for case 1, Eq. (B1) is applied at each external boundary, $j=0$ and J (Fig. 2a without opaque layers). The boundary conditions in Eqs. (3a) and (3b) are used to eliminate the resulting unknown external temperature on each side (at $j=-1$ and $J+1$) according to the following development. At $X=0$, where $j=0$, Eq. (B1) gives

$$t_{j=0,n+1} = t_{j=0,n} + \frac{N_c\Delta\upsilon}{\Delta X^2}(t_{j=1,n} - 2t_{j=0,n} + t_{j=-1,n}) - \frac{\Delta\upsilon}{4}\frac{\partial\tilde{q}_r}{\partial X}\bigg|_{j=0,n} \tag{B2a}$$

where $t_{j=-1,n}$ is found from the boundary condition Eq. (3a) as

$$t_{j=-1,n} = t_{j=1,n} + (\Delta X/2N_c)H_1(t_{g1} - t_{j=0,n}) \tag{B2b}$$

Similarly at $X=1$,

$$t_{j=J,n+1} = t_{j=J,n} + \frac{N_c\Delta\upsilon}{\Delta X^2}(t_{J+1,n} - 2t_{J,n} + t_{J-1,n}) - \frac{\Delta\upsilon}{4}\frac{\partial\tilde{q}_r}{\partial X}\bigg|_{j=J,n} \tag{B3a}$$

where $t_{J+1,n}$ is found from

$$t_{J+1,n} = t_{J-1,n} + (\Delta X/2N_c)H_2(t_{g2} - t_{J,n}) \tag{B3b}$$

For case 2, Eq. (B2) applies at $X=0$, where the translucent boundary is directly exposed to the environment. At $X = x/\delta_c = 1$, the translucent layer is in contact with a thin metal layer that has a temperature distribution assumed to be uniform throughout its thickness at each time. At this internal interface, such as at point J in Fig. 2a, the temperatures are equal for the translucent material and the metal. The finite difference relation at $j=J$ is developed by considering the half-element $\Delta x/2$ as in Fig. 2a. The energy entering the translucent layer from the opaque layer was considered in the boundary condition Eq. (4b). The heat balance for the translucent element includes heat conduction from the adjacent translucent material, radiative absorption and emission at both metal surfaces, convection to the external surface of the metal, the volumetric radiative heat source in the half-increment of the translucent layer adjacent to the interface, the heat capacity of the thin metal layer, and the heat capacity of the half-increment of the translucent material adjacent to the interface. The individual terms are developed as follows. For time increment $\Delta\theta$, the change in heat capacity of the thin metal layer and the adjacent half-increment of the translucent material is

$$[\rho_c c_c(\Delta x/2) + \rho_m c_m\delta_m](T_{J,n+1} - T_{J,n})$$

The heat addition to the element by heat conduction from the adjacent translucent material and by convection and radiation at the external metal boundary is

$$\Big[(k_c/\Delta x)(T_{J-1,n} - T_{J,n}) + h_2\big(T_{g2} - T_{J,n}\big) + \epsilon_{mo}(q_{r2} - \sigma T_{J,n}^4)\Big]\Delta\theta$$

The radiative internal heat source in the half-element of the translucent material is

$$-\frac{\Delta x}{2}\Delta\theta\frac{\partial q_r}{\partial x}\bigg|_{x=\delta_c - \Delta x/4}$$

The radiative energy absorbed at the inside surface of the opaque wall is equal to the net radiative flux in the x direction (the difference between incident and leaving fluxes). This is obtained from the boundary condition in Eq. (5b) and the relation between G and q_r as

$$q_r(\delta_c, \theta)\Delta\theta = -\frac{1}{3(a+\sigma_s)}\frac{\partial G(x, \theta)}{\partial x}\bigg|_{x=\delta_c}\Delta\theta = \frac{\epsilon_{mi}}{2-\epsilon_{mi}}\left[\frac{G(\delta_c, \theta)}{2} - 2n^2\sigma T_c^4(\delta_c, \theta)\right]\Delta\theta$$

Using these terms to form a heat balance and then placing the results in dimensionless form yields the finite difference equation at grid point J:

$$t_{J,n+1} = t_{J,n} + \left[\Delta\upsilon\Big/\left(\frac{\Delta X}{2} + C_{mc}\frac{\delta_m}{\delta_c}\right)\right]\left[\frac{N_c}{\Delta X}(t_{J-1,n} - t_{J,n}) + \frac{H_2}{4}(t_{g2} - t_{J,n}) + \frac{\epsilon_{mo}}{4}\big(\tilde{q}_{r2} - t_{J,n}^4\big) + \frac{1}{2R_m}\left(\frac{\tilde{G}_{J,n}}{4} - n^2 t_{J,n}^4\right) - \frac{\Delta X}{8}\frac{\partial\tilde{q}_r}{\partial X}\bigg|_{1-\Delta X/4}\right] \tag{B4}$$

For case 3, which applies for Figs. 1c and 1d, a relation must be written for the first grid point at the interface of the translucent material with the thin metal layer at $X = 0$ and if there are two translucent layers, for the temperature at and within the internal metal layer. Similar to Eq. (B4), the relation at $X = 0$ is

$$t_{0,n+1} = t_{0,n} + \left[\Delta\upsilon \Big/ \left(\frac{\Delta X}{2} + C_{mc}\frac{\delta_m}{\delta_c}\right)\right]\left[\frac{N_c}{\Delta X}(t_{1,n} - t_{0,n}) + \frac{H_1}{4}(t_{g1} - t_{0,n}) + \frac{\epsilon_{mo}}{4}\left(\tilde{q}_{r1} - t_{0,n}^4\right) + \frac{1}{2R_m}\left(\frac{\tilde{G}_{0,n}}{4} - n^2 t_{0,n}^4\right) - \frac{\Delta X}{8}\frac{\partial \tilde{q}1_r}{\partial X}\bigg|_{\Delta X/4}\right] \tag{B5}$$

where $-\partial\tilde{q}1_r/\partial X$ is the radiative heat source in the translucent layer on the left in Fig. 1d. For the opaque layer between two translucent layers, it is necessary to include absorption and emission from both sides of the metal, the radiative volumetric heat sources in the half-increments of the translucent layers on both sides, and the heat capacity of these half-increments and of the metal. By the use of the ideas in the preceding derivation, this yields the relation

$$t_{J,n+1} = t_{k=0,n+1} = t_{J,n} + \left[\Delta\upsilon \Big/ \left(\Delta X + C_{mc}\frac{\delta_m}{\delta_c}\right)\right] \times \left[\frac{N_c}{\Delta X}(t_{J-1,n} - 2t_{J,n} + t_{k=1,n}) - \frac{\Delta X}{8}\frac{\partial \tilde{q}1_r}{\partial X}\bigg|_{1-\Delta X/4} + \frac{1}{R_m}\left(\frac{\tilde{G}_{J,n} + \tilde{G}_{k=0,n}}{8} - n^2 t_{J,n}^4\right) - \frac{\Delta X}{8}\frac{\partial \tilde{q}2_r}{\partial X}\bigg|_{\Delta X/4}\right] \tag{B6}$$

where $\tilde{q}1_r$ and $\tilde{q}2_r$ are in the translucent layers on the left and right sides of the internal opaque layer.

References

[1] Siegel, R., and Spuckler, C. M., "Analysis of Thermal Radiation Effects on Temperatures in Turbine Engine Thermal Barrier Coatings," *Materials Science and Engineering A*, Vol. A245, No. 2, 1998, pp. 150–159.

[2] Wahiduzzaman, S., and Morel, T., "Effect of Translucence of Engineering Ceramics on Heat Transfer in Diesel Engines," Oak Ridge National Lab. Rept. ORNL/Sub/88-22042/2, Oak Ridge, TN, April 1992.

[3] Siegel, R., "Transient Thermal Effects of Radiant Energy in Translucent Materials," *Journal of Heat Transfer*, Vol. 120, No. 1, 1998, pp. 4–23.

[4] Tsai, C.-F., and Nixon, G., "Transient Temperature Distribution of a Multilayer Composite Wall with Effects of Internal Thermal Radiation and Conduction," *Numerical Heat Transfer*, Vol. 10, No. 1, 1986, pp. 95–101.

[5] Ho, C.-H., and Özişik, M. N., "Combined Conduction and Radiation in a Two-Layer Planar Medium with Flux Boundary Condition," *Numerical Heat Transfer*, Vol. 11, No. 2, 1987, pp. 321–340.

[6] Glass, D. E., Özişik, M. N., and McRae, D. S., "Combined Conduction and Radiation with Flux Boundary Condition for a Semi-Transparent Medium Covered by Thin Radiating Layers," *Journal of Quantitative Spectroscopy and Radiative Transfer*, Vol. 38, No. 3, 1987, pp. 201–208.

[7] Siegel, R., "Two-Flux and Green's Function Method for Transient Radiative Transfer in a Semitransparent Layer," *Radiative Transfer I, Proceedings of the 1st International Symposium on Radiative Transfer*, Begell, New York, 1996, pp. 473–487.

[8] Siegel, R., "Green's Function to Determine Temperature Distribution in a Semitransparent Thermal Barrier Coating," *Journal of Thermophysics and Heat Transfer*, Vol. 11, No. 4, 1997, pp. 315–318.

[9] Siegel, R., "Temperature Distribution in a Composite of Opaque and Semitransparent Spectral Layers," *Journal of Thermophysics and Heat Transfer*, Vol. 11, No. 4, 1997, pp. 533–539.

[10] Siegel, R., and Howell, J. R., *Thermal Radiation Heat Transfer*, 3rd ed., Hemisphere, Washington, DC, 1992, pp. 691–695.